Spin-resonance modes of the spin-gap magnet $TlCuCl_3$

V. N. Glazkov* and A. I. Smirnov
P. L. Kapitza Institute for Physical Problems RAS, 117334 Moscow, Russia

H. Tanaka and A. Oosawa
Department of Physics, Tokyo Institute of Technology, Meguro-ku, Tokyo 152-8551, Japan
(Received 21 November 2003; revised manuscript received 3 March 2004; published 19 May 2004)

Three kinds of magnetic-resonance signals were detected in crystals of the spin-gap magnet $TlCuCl_3$. First, we have found antiferromagnetic resonance absorption in the field-induced antiferromagnetic phase above the critical field H_c. This resonance frequency is strongly anisotropic with respect to the direction of the magnetic field. The field dependence of the induced order parameter is determined. Second, we have observed the microwave absorption due to the transitions between the singlet ground state and the excited collective triplet states. Finally, the thermally activated resonance absorption due to the transitions between the spin sublevels of the triplet excitations was found. These sublevels are split by the crystal field and external magnetic field.

DOI: 10.1103/PhysRevB.69.184410 PACS number(s): 75.10.Jm, 75.50.Ee, 76.50.+g

I. INTRODUCTION

The spin-gap magnets have been intensively studied during last decades because of various quantum-disordered states found there. The spin-gap structures were found in one-dimensional (1D) antiferromagnets such as dimerized spin $S=1/2$ chains, including spin-Peierls magnets,[1] spin $S=1$ chains,[2] spin ladders,[3] and in dimer structures.[4] While the disordered ground states of spin-gap systems are stable with respect to a weak interchain exchange or anisotropy, the spin-gap systems demonstrate an antiferromagnetic ordering induced by weak doping[5] or by a strong magnetic field.[6] Impurities destroy locally the spin-gap state and restore a local antiferromagnetic order around impurity atoms. The overlapping of these ordered areas in the presence of a weak interchain exchange results in a long-range magnetic order. Magnetic field closes the spin gap, making an ordered state possible. The spin-gap magnet $TlCuCl_3$ is a unique compound demonstrating both an impurity-induced ordering in zero field[7] and a field induced ordering in pure crystals.[6,8]

The crystals of $TlCuCl_3$ have a dimer spin structure formed by the $S=1/2$ spins of Cu^{2+} ions. The dimers construct infinite double spin chains coupled to each other, thus the system is a strongly coupled 3D dimer network. The spin-gap spectrum of excitations was found in Ref. 9. The structure of exchange interactions, derived from neutron-scattering experiments, is described in Ref. 10: the strongest antiferromagnetic exchange is within the chemical dimer Cu_2Cl_6 (5.68 meV), the spin-gap value is 0.65 meV.

The field-induced antiferromagnetic ordering was found in a magnetic field $H>H_c\sim 50$ kOe in measurements of the magnetization.[6] Formation of the field-induced long-range magnetic order was confirmed by neutron-scattering experiments.[8] The transition field has a strong temperature dependence.[6,11] This dependence, unexpected in the mean-field theory, was qualitatively described in the model of Bose-Einstein condensation (BEC) of magnons.[12] The applicability of the BEC model to the field-induced phase transitions in the spin-gap materials is rigorously valid only in case of rotational symmetry around the field direction. One of the consequences of rotational symmetry is the existence of the gapless Goldstone mode above the H_c.

High-frequency magnetic-resonance measurements[13,14] have demonstrated directly the field dependence of the energy gap, but were limited to the fields $H<H_c$ and a few number of microwave frequencies. The energy of zero-momentum magnetic excitations was measured in a wide range of magnetic fields in the neutron-scattering investigation.[15] The closing of the spin gap in the magnetic field $H=H_c$ was confirmed, but the excitations below 0.75 meV (176 GHz) could not be resolved at $H>H_c$ because of the strong magnetic Bragg reflection. Thus, no low-frequency response was found in the field range above H_c, and it was suggested that the energy of the lowest excitations is zero at $H>H_c$, in accordance with the BEC model prediction.

In the present paper we describe the detailed magnetic-resonance study of the single-crystal samples of $TlCuCl_3$ in the range of microwave frequencies 9–80 GHz, in magnetic fields up to 80 kOe. We detected the magnetic-resonance signals in the field-induced ordered phase and measured their frequency-field dependences, which appeared to be nonlinear and strongly anisotropic with respect to the direction of the magnetic field. This observation evidences that lowest excitation in the field-induced ordered phase is non-Goldstone mode. Besides, in the low-field range, we observed the microwave absorption due to the transitions between the ground state and the excited triplet states. Finally, we found electron-spin-resonance (ESR) signals of the thermally excited triplet excitations. This kind of resonance is due to the transitions between the spin sublevels of triplet states. The evolution of triplet split spectrum to a single exchange narrowed line was observed.

II. SAMPLES AND EXPERIMENTAL DETAILS

The crystals of $TlCuCl_3$ have monoclinic symmetry with the space group C_{2h}^5 $(P2_1/c)$. The twofold axis is denoted as b. The axes a and c form an angle of 96.32°.

The sample growth is described in details in Ref. 6. Crys-

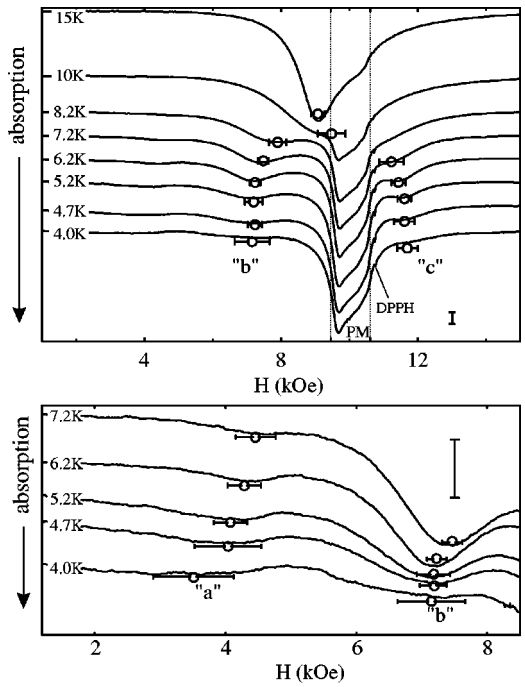

FIG. 1. Temperature evolution of the low-field part of the ESR spectrum at $\mathbf{H}\perp(10\bar{2})$ and $f=30.05$ GHz. Lower panel represents a blowup of the data (vertical bar on both panels has the same absolute value). Letters "*a*,""*b*,""*c*" denote thermally activated components of the ESR spectrum. Circles with error bars mark values of the resonance fields for components "*b*" and "*c*." Absorption signal marked as PM is due to the parasitic hydratation of the sample surface. The narrow line on the right wing of the PM signal is the diphenylpicrylhydrazyl-mark ($g=2.0$).

tals have cleavage planes (010) and $(10\bar{2})$. During our experiments we have mounted crystals in the following mutually perpendicular orientations with respect to the magnetic field: $H\|[010]$ (b axis), $H\perp(10\bar{2})$, and $H\|[201]$. The [201] direction forms an angle of 51.4° with the a axis and an angle of 44.92° with the c axis. We have used single crystals with the volume of about ~ 20–50 mm^3. The crystals are hygroscopic, and a hydrated phase was present on the surface of the samples, giving a parasitic paramagnetic resonance signal, this signal grew when samples were exposed at open atmosphere.

ESR spectra were taken by means of a set of home made microwave spectrometers with transmission-type cavities and a superconducting magnet. The frequency range of the apparatus is 9–100 GHz. ESR spectra were recorded as field dependences of the microwave power transmitted through the cavity with the sample.

III. EXPERIMENTAL RESULTS

A. ESR at different temperatures

The temperature evolution of an ESR absorption curve in the low-field range is presented in Figs. 1 and 2, the high-field data are illustrated in Fig. 3. The absorption spectrum consists of several components with different temperature dependences of the intensity and of the resonance field.

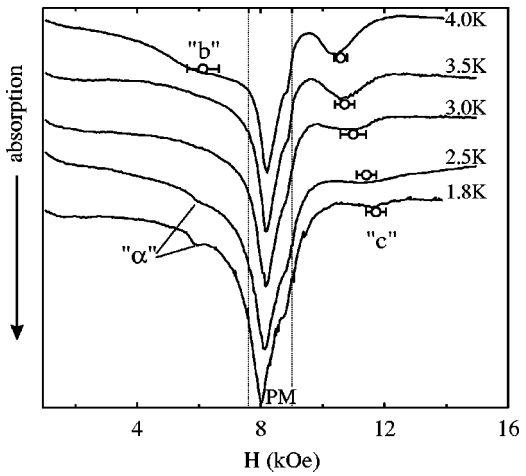

FIG. 2. Evolution of the low-field ESR spectrum below $T=4.2$ K at $\mathbf{H}\|b$, $f=25.94$ GHz. "*b*" and "*c*" mark thermally activated ESR components, "α" is a weak paramagnetic signal with $g\approx 3$. Circles with error bars mark resonance fields for components "*b*" and "*c*."

At first, there are several components located near the paramagnetic resonance field (e.g., near 10 kOe for the microwave frequency $f=30.05$ GHz, as shown on Fig. 1). The parasitic absorption occurs in the field range marked as PM, and has the Curie-like behavior of the integrated intensity. The shape of this absorption curve is typical for powder samples, with two sharp boundaries originating from the maximum and minimum values of an anisotropic g factor. The line shape and position of this absorption do not depend on the orientation of the magnetic field with respect to crystal axes. From the intensity of the paramagnetic resonance signal of the hydrated surface we estimate the number of the paramagnetic ions in this spoiled area of the crystal as 0.02 from the total number of magnetic ions.

Apart from the parasitic signal, we observe thermally activated resonance absorption (lines marked in order of their resonance field increase as "*a*," "*b*," and "*c*," see Fig. 1). The resonance fields of these components are temperature

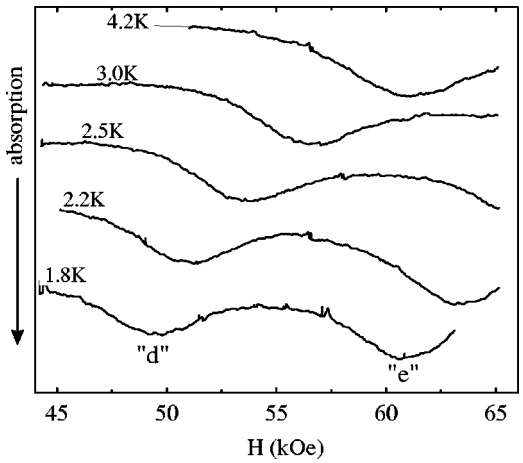

FIG. 3. Temperature evolution of the high-field ESR spectrum at $\mathbf{H}\|b$, $f=25.94$ GHz. Letters "*d*,""*e*" mark spectral components.

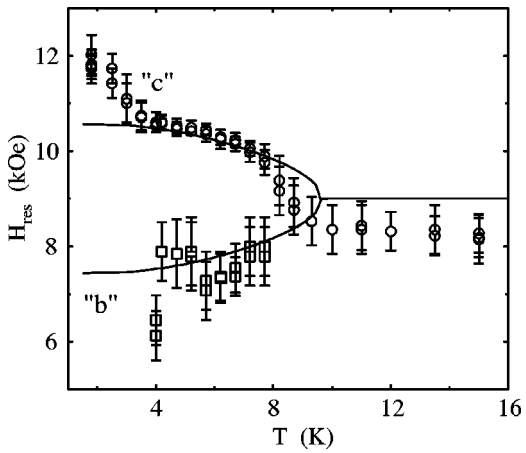

FIG. 4. Temperature dependences of the ESR fields of components "*b*" and "*c*" at $\mathbf{H}\|b$, $f=25.94$ GHz. Solid curves represent exchange narrowing theory (see text).

dependent, they become closer to each other as temperature rises and finally coalescence into a single line at $T\approx 8$ K. As expected for Cu^{2+} ions, the g factor of this single line is close to 2.0 and its anisotropy does not exceed 15%. At low temperature the resonance field of the component "*a*" is close to a half of the resonance field of free spins $H_f = hf/g\mu_B H$ (f is the microwave frequency), and the resonance fields of components "*b*" and "*c*" are located on both sides from H_f. The splitting of the single resonance line into several components with decreasing temperature was observed for all three orientations of the applied magnetic field. However, the half-field absorption component "*a*" was not observed for $\mathbf{H}\|b$, and the component "*b*" cannot be resolved on the background of the strong parasitic paramagnetic absorption for $\mathbf{H}\|[201]$. The temperature dependences of resonance fields and intensities for thermally activated components are given in Figs. 4 and 5. The "*a*" component intensity is small, the most part of the ESR intensity is concentrated in "*b*" and "*c*" components. The intensities of these components are slightly different (this difference is of

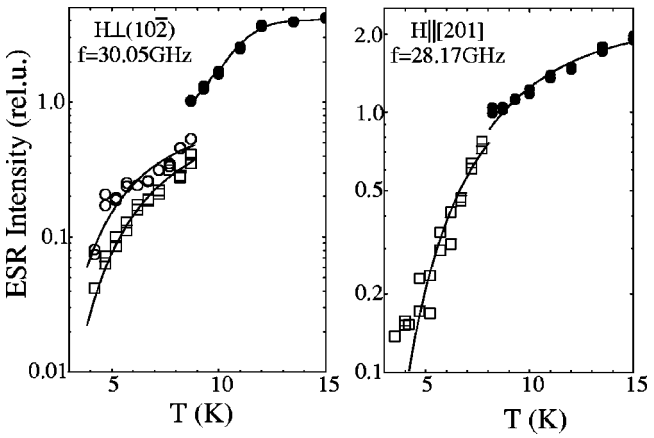

FIG. 5. Temperature dependence of the ESR integrated intensity. Symbols: filled circles, exchange narrowed ESR line above the splitting temperature; open circles, component "*b*" squares, component "*c*." Curves are guide to the eye.

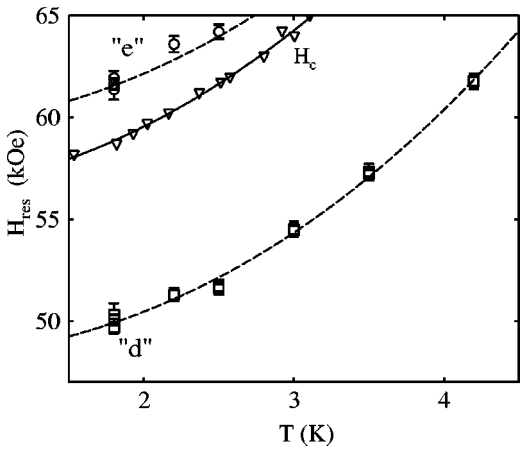

FIG. 6. Temperature dependences of the ESR fields for the high-field components "*d*" and "*e*" at $\mathbf{H}\|b$, $f=25.94$ GHz. Circles, component "*e*"; squares, component "*d*"; triangles, $H_c(T)$ data from Ref. 11. Curves are guide to the eye.

about of 10% of the total intensity). The position of the more intensive component is orientation dependent: for $\mathbf{H}\perp(10\bar{2})$ the "*b*" component is more intensive, while for $\mathbf{H}\|[201]$ the "*c*" component conserves more then a half of the total intensity when measured at the temperature of splitting. The intensities of components "*a*," "*b*," "*c*" decrease quickly with decreasing temperature, practically disappearing near 1.5 K.

The ESR absorption in the high-field range (Fig. 3) was observed only at temperatures below 4.2 K. Here the absorption line consists of the two components marked by the letters "*d*" and "*e*," located on both sides of the critical field H_c. Both components shift to the higher fields with temperature increase (see Fig. 6), in accordance with the increase of the critical field H_c.[11]

B. Magnetic-resonance spectra

ESR absorption lines taken at different frequencies are presented in Fig. 7. The changing of the resonance fields of the components "*a*," "*c*," and "*d*" is visible here. Besides these regular components there are weak components "α" and "β" with a paramagnetic behavior of the intensity. We ascribe these components to a small amount of impurities or parasitic phases.

The measured field dependences of ESR frequencies for three perpendicular orientations of the magnetic field [$\mathbf{H}\|b$, $\mathbf{H}\perp(10\bar{2})$, and $\mathbf{H}\|[201]$] are given in Figs. 8–10.

The resonance fields of thermally activated components "*a*," "*b*," and "*c*" increase with the increase of the microwave frequency. ESR lines "*b*" and "*c*" show linear $f(H)$ dependences. However, the linear extrapolation of their resonance frequencies to zero field results in nonzero values. The magnitude of the splitting between "*b*" and "*c*" components is of about 10 GHz. The fine details of the frequency-field dependences of thermally activated components measured at two temperatures 4.2 K and 1.5 K are shown in the Fig. 11. Note that for the observation of the ESR signals from noninteracting triplet excitations (at small population numbers)

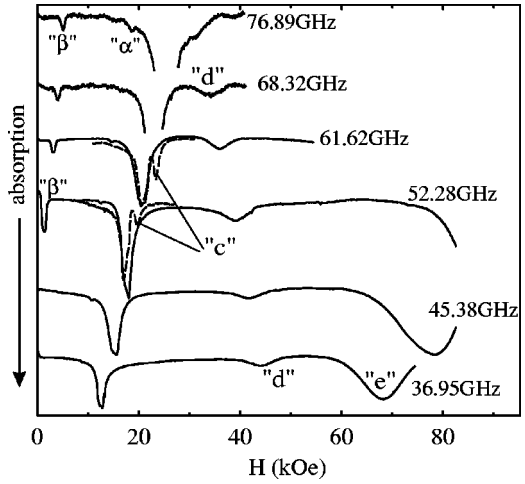

FIG. 7. ESR spectra at different frequencies for $\mathbf{H}\|b$. Solid lines, $T=1.5$ K; dashed lines, $T=4.2$ K. Intensive signals of the paramagnetic absorption at $f=76.89$ GHz and $f=68.32$ GHz are partially removed. Letters mark different spectral components as described in the text.

we have to deal at the lowest temperature. From the other side, the freezing out of the intensity of these components complicates the detection of signals and the measurement of resonance fields. At both temperatures the observed ESR frequencies of the "*b*" and "*c*" spectral components may be described well by the linear equation

$$f=\frac{g\mu_B H}{h}\pm A. \tag{1}$$

The fitting procedure according to Eq. (1) for temperature independent but anisotropic g factor, and temperature-dependent constants A results in the following values:

$$\mathbf{H}\perp(10\bar{2}):g=2.30\pm0.05,\quad A(4.2\ \text{K})=6.8\pm1.0\ \text{GHz},$$

$$A(1.5\ \text{K})=12\pm2\ \text{GHz}$$

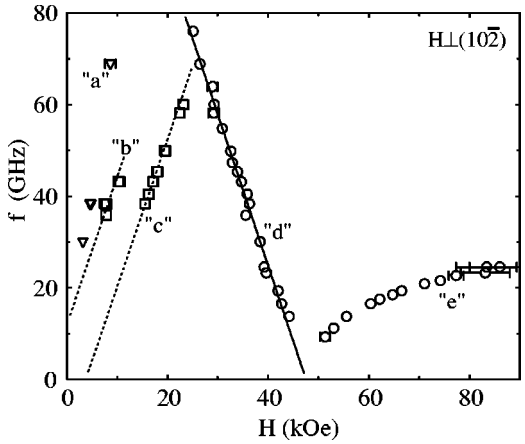

FIG. 8. Frequency-field dependences for spectral components "*a*"–"*e*" taken at $\mathbf{H}\perp(10\bar{2})$ and $T=1.5$ K. Lines are linear fits with parameters described in the text.

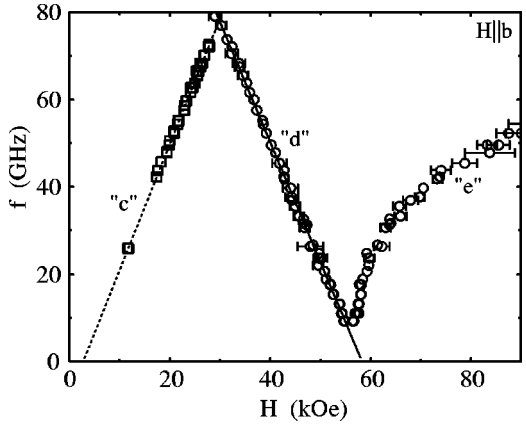

FIG. 9. Frequency-field dependences for spectral components "*c*"–"*e*" taken at $\mathbf{H}\|b$ and $T=1.5$ K. Lines are linear fits with parameters described in the text.

$$\mathbf{H}\|b:g=2.06\pm0.02,\quad A(4.2\ \text{K})=4.5\pm0.5\ \text{GHz},$$

$$A(1.5\ \text{K})=8.0\pm0.7\ \text{GHz},$$

$$\mathbf{H}\|[201]:g=2.03\pm0.02,\quad A(4.2\ \text{K})=2.6\pm0.4\ \text{GHz},$$

$$A(1.5\ \text{K})=3.9\pm0.5\ \text{GHz}.$$

The correspondence of the fitting dependences and experimentally observed frequencies illustrated in Fig. 11 is quite satisfactory. The g-factor values determined from the fitting of the split low-temperature spectra coincides within the experimental error with the g values measured above 10 K, as well as with the g-factor values measured in Ref. 6 ($g_b=2.06$, $g_{\perp(10\bar{2})}=2.23$).

High-field absorption components "*d*" and "*e*" differ strongly in their frequency-field dependences. The resonance "*d*" (to the left of the critical field H_c) linearly shifts to lower fields at the frequency increase. This ESR mode can be identified as absorption due to the transitions between singlet ground state and gapped triplet states, analogous to the ab-

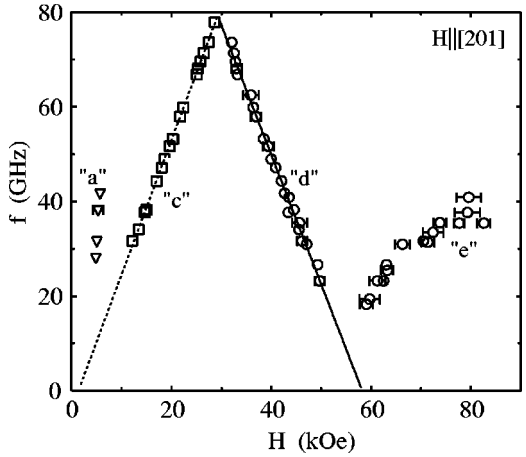

FIG. 10. Frequency-field dependences for spectral components "*a*," "*c*"–"*e*" taken at $\mathbf{H}\|[201]$ and $T=1.5$ K. Lines are linear fits with parameters described in the text.

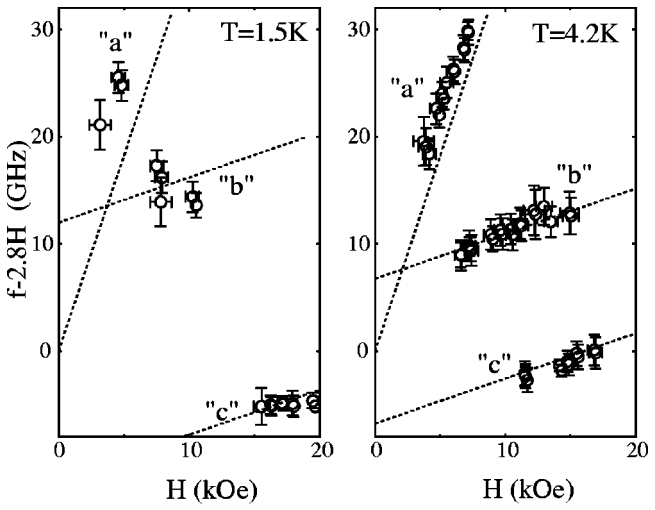

FIG. 11. ESR spectra of the triplet excitations at $\mathbf{H}\perp(10\bar{2})$, $T=1.5$ K (left), and $T=4.2$ K (right). The linear contribution, corresponding to the $g=2.0$ ESR is subtracted. Lines present the linear approximation (see text).

sorption observed in Refs. 13 and 14 The frequency of this component agrees well with the energy of the lowest triplet states measured by neutron scattering.[15] The component *"e"* shifts to the higher fields with increasing frequency, its frequency-field dependence is nonlinear and anisotropic with respect to the orientation of the external field. This resonance mode was not reported in previous investigations.

IV. DISCUSSION

A. ESR of the triplet excitations

The thermal activation of the absorption lines *"a,""b,""c"* indicates that they are due to the gapped triplet excitations. The growth of intensity of these components beginning at $T\simeq 4$ K correlates well with the growth of the susceptibility measured in Ref. 6 and with the gap value 7.7 K. A remarkable feature of the observed triplet ESR is the splitting of this resonance into two components, and arising of a weak component *"a."*

While the magnetic-resonance frequency of isolated $S=1/2$ Cu^{2+} ions is not affected by the crystal field, the collective excitations of a system of exchange-coupled Cu^{2+} ions are triplets carrying spins $S=1$. Therefore, the magnetic-resonance frequency of triplets should be influenced by a crystal field. The crystal field splits magnetic sublevels of a spin $S=1$ state even at zero magnetic field.[16] This splitting results in a three-component spectrum, corresponding to the transitions between different pairs of the spin sublevels.Thus, we interpret the observed lines *"a,""b,""c"* as absorption due to transitions between the sublevels of triplet excitations.

The coalescence of the ESR line components at the temperature increase corresponds to the scenario of the formation of the exchange narrowed ESR line (see, e.g., Ref. 17): when the exchange interaction between the spins precessing with different frequencies is weak (slow exchange limit), there are separate modes of magnetic resonance. For the opposite limit, when the exchange frequency is greater than the difference in eigenfrequencies, a single collective mode is formed, known as exchange-narrowed mode. For thermally activated spins the exchange frequency is temperature dependent. The scenario with the transition from the slow to the fast limit of the exchange narrowing of ESR lines was observed earlier, e.g., in magnetic-resonance study of molecules with thermally activated spin states[18] and at the temperature evolution of the ESR spectra of the spin-Peierls magnet $CuGeO_3$ doped with impurities.[19,20] The observed evolution of the triplet ESR lines in $TlCuCl_3$ follows the same scenario. At low temperatures the concentration of triplets is small and three-component ESR of noninteracting triplets with spin $S=1$ in a crystal field is observed. At the larger concentration of activated spins (at higher temperatures) the components merge in a single ESR line.

Starting from this qualitative consideration of thermally activated resonances we can further describe on a quantitative level the ESR frequencies at low temperature and the temperature evolution. The ESR frequencies are explained (see, e.g., Ref. 21) by assuming an effective Hamiltonian for the triplet with the wave vector $\mathbf{k}$ given by

$$\mathcal{H}_{\mathbf{k}}=\mu_B\mathbf{S}\hat{g}\mathbf{H}+D_{\mathbf{k}}S_z^2+E_{\mathbf{k}}(S_x^2-S_y^2)+\Delta_{\mathbf{k}}. \qquad (2)$$

Here $\hat{g}$ is a g tensor, $\Delta_{\mathbf{k}}$ is the energy of the triplet excitation with the wave vector $\mathbf{k}$ in absence of the magnetic-field and crystal-field anisotropy, $D_{\mathbf{k}},E_{\mathbf{k}}$ are the anisotropy constants. The anisotropy constants may be $\mathbf{k}$ dependent, as, e.g., in a Haldane magnet.[22]

The triplet excitations are multispin objects, hence, the symmetry of the effective crystal field should be determined by the crystal symmetry and not by the symmetry of the local surrounding of the magnetic ions. Thus, one axis of the symmetry of the effective field should be aligned along the twofold axis b, we note it as $\mathbf{z}\|b$. The other two axes lie within the $a-c$ plane of the crystal. We suppose that the x axis is directed along the direction of transverse spin ordering at $\mathbf{H}\|b$, i.e., at an angle of 39° from the a axis in the a-c plane.[8]

The scheme of the energy levels of the spin-gap system in the magnetic field for $\mathbf{k}=0$ is shown in Fig. 12. Possible ESR transitions are shown by arrows. These are: (i) transitions between different components of the triplet, (ii) transition from the singlet ground state to the excited triplet state below H_c, (iii) transition from the ordered ground state at $H>H_c$ to the lowest excited state.

Note that in the isotropic exchange approximation, the singlet-triplet transitions may not be excited by the oscillating magnetic field, because for the states belonging to different multiplets the appropriate matrix element is zero. Anisotropic interactions will allow this excitation. The two-quantum intratriplet transition between states with $S_z=\pm 1$ is forbidden if the direction of the external magnetic field coincides with one of the anisotropy axes. Wave vector selection rules allow intratriplet transitions for thermally excited triplets with any $\mathbf{k}$ value, thus the observed transitions between the sublevels of the triplet excitations are integrated

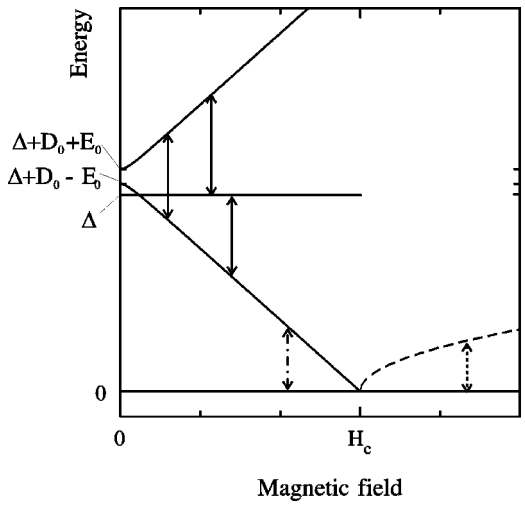

FIG. 12. Scheme of the energy levels of the spin-gap system in the magnetic field in the presence of the orthorhombic anisotropy. Arrows show possible ESR transitions: intratriplet (solid), singlet-triplet (dash-dotted), transition above H_c (dotted). $\mathbf{H}\|z$, $\mathbf{k}=0$.

over the thermally excited ensemble of the triplet excitations. The singlet-triplet transitions may be observed only for zero-**k** triplets. In the ordered state above H_c the transitions from the ground state to the zero-**k** excitations are allowed.

Considering the anisotropy terms as a perturbation to the Zeeman term, in the first order of the perturbation theory one obtains for the energy levels

$$E_{\pm}=\pm g_{\alpha}\mu_B H+\frac{D_{\mathbf{k}}}{2}[(\mathbf{z}\cdot\mathbf{n})^2+1]+\frac{E_{\mathbf{k}}}{2}[(\mathbf{x}\cdot\mathbf{n})^2-(\mathbf{y}\cdot\mathbf{n})^2]+\Delta_{\mathbf{k}}, \tag{3}$$

$$E_0=D_{\mathbf{k}}[1-(\mathbf{z}\cdot\mathbf{n})^2]-E_{\mathbf{k}}[(\mathbf{x}\cdot\mathbf{n})^2-(\mathbf{y}\cdot\mathbf{n})^2]+\Delta_{\mathbf{k}}. \tag{4}$$

Here g_{α} is the g-factor value for the corresponding direction of magnetic field and **n** is the unit vector parallel to the magnetic field.

The spectrum of the observed thermally activated absorption should be determined by the anisotropy constants $D_{\mathbf{k}}$, $E_{\mathbf{k}}$ averaged over the ensemble of triplet excitations at given temperature. Thus, the values D and E, resulting from the averaging of $D_{\mathbf{k}}$ and $E_{\mathbf{k}}$, turn out to be temperature dependent. The averaged transition frequencies are

$$\hbar\omega_{1,2}=g_{\alpha}\mu_B H\pm\left[\frac{D}{2}[3(\mathbf{z}\cdot\mathbf{n})^2-1]+\frac{3E}{2}[(\mathbf{x}\cdot\mathbf{n})^2-(\mathbf{y}\cdot\mathbf{n})^2]\right], \tag{5}$$

$$\hbar\omega_3=2g_{\alpha}\mu_B H. \tag{6}$$

The resonance frequencies $\omega_{1,2}$ demonstrate linear frequency-field dependences shifted upward or downward from the $S=1/2$ ESR frequency $\omega=g\mu_B H/\hbar$. These modes correspond to the observed ESR lines "b" and "c." The resonance field of the third resonance mode ω_3 should be equal to the half of the normal ESR field H_f. This mode corresponds to the line "a." The absolute value of the deviation of resonance frequencies $2\pi\omega_{1,2}$ from the free spin-resonance frequency $g\mu_B H/h$ for one of the three arbitrary mutually orthogonal directions of the external field equals to the sum of the absolute values of deviations for two other directions. This relation is valid for the measured deviations A, confirming that the observed splitting is due to the crystal field. The low-field absorption component "a" was not observed for $\mathbf{H}\|b$, which is also in agreement with the above-formulated selection rules for the transitions between the sublevels of the triplet excitations in the crystal field.

The values of the anisotropy constants can be deduced from the observed values of A by means of Eq. (5). To determine the signs of anisotropy constants, one should consider that at $g\mu_B H\gg D,E$ the absorption due to the transitions $|-\rangle\leftrightarrow|0\rangle$ is larger than that due to the transitions $|+\rangle\leftrightarrow|0\rangle$. The determined values are at

$$T=1.5\text{ K}: D/h=8.0\pm0.7\text{ GHz},\quad E/h=5.8\pm0.6\text{ GHz},$$

and at

$$T=4.2\text{ K}: D/h=4.5\pm0.5\text{ GHz},\quad E/h=3.6\pm0.5\text{ GHz}.$$

The observed change of the anisotropy constants D and E with temperature probably indicates the change of the distribution of the thermally excited triplet excitations in the phase space. At low temperature $T=1.5$ K the triplets are excited mainly near the bottom of the triplet band, while at $T=4.2$ K (this temperature corresponds to one half of the spin-gap energy) the triplets are excited over the whole band.

The temperature evolution of the thermally activated lines, shown in Fig. 4, may be analyzed using the approach of the exchange narrowed spin resonance.[17] We neglect here the intensity of the almost prohibited two-quantum component "a," and the difference between the intensities of components "b" and "c." The frequency shift δf from the center of gravity of the ESR spectrum is given by the exchange narrowing theory:[17]

$$f_e>f_0:\delta f=0, \tag{7}$$

$$f_e<f_0:\delta f=\pm\sqrt{f_0^2-f_e^2}. \tag{8}$$

Here $\pm f_0$ are the deviations of the resonance frequencies from the center of gravity of the ESR spectrum in the absence of the exchange narrowing, and f_e is the average exchange frequency.

For thermally excited magnetic states, the exchange frequency is temperature dependent,[18]

$$f_e=F\ \exp\left(-\frac{\Delta}{k_B T}\right). \tag{9}$$

Here $\Delta=7.7$ K is a zero-field energy gap.

The theoretical curves, calculated using Eqs. (7)–(9), are shown in Fig. 4. We have taken the splitting value f_0 to be equal to splitting at 4.2 K and used preexponential factor F

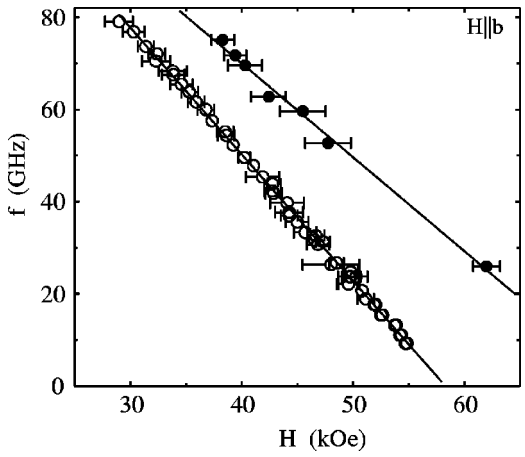

FIG. 13. The frequency-field dependence for for the singlet-triplet transition. Open symbols, $T=1.5$ K; closed, $T=4.2$ K. $\mathbf{H}\|b$.

as a fitting parameter. The fitting curves presented by solid lines in Fig. 4 correspond to the value $F=10$ GHz.

The model of the exchange narrowing used here is simplified. First, it does not include the temperature dependence of the effective anisotropy constants D and E. Another simplification is ignorance of the field dependence of the energy gap and of the different population numbers of energy levels. Particularly, this simplified model can not explain the abrupt change of the resonance frequency of component "*b*" between the temperatures 1.5 and 4 K. Probably, this change is due to the expanding of the phase space occupied by the excited triplets at $T>\Delta/2=4$ K, resulting in change of the effective constants D and E.

B. Singlet-triplet transitions

The ESR component "*d*" corresponds to direct over-gap transitions between singlet ground state and gapped triplet states. In the isotropic Heisenberg approximation these transitions cannot be excited by the microwave field. Nevertheless, the anisotropic interactions resulting in the effective Hamiltonian (2) will allow these transitions. The same type of ESR absorption was reported earlier for higher frequencies.[13,14] The ESR spectrum of this component may be described by the linear equation

$$f=\frac{1}{h}(\tilde{\Delta}-\tilde{g}\mu_B H). \tag{10}$$

Here $\tilde{\Delta}$ is expected to be close to the spin gap Δ and $\tilde{g}$ is the effective g factor.

The straight lines on Figs. 8, 9, and 13 present results of the linear fitting according to the relation (10) with the parameters given in Table I.

The value $\tilde{\Delta}$ obtained from linear extrapolation corresponds well to the value of 156 GHz observed in other ESR (Refs. 13,14) and neutron studies.[15] The effect of the crystal field discussed in the preceding section should result in the splitting of the zero-field energy level Δ into three sublevels: Δ, $\Delta+D_0-E_0$, and $\Delta+D_0+E_0$ (see Fig. 12, an analogous energy-level diagram is given in Ref. 21). The $f(H)$ curves

TABLE I. Effective g factors and spin gaps.

		$\tilde{g}$	$\tilde{\Delta}/h$, GHz
$T=1.5$ K	$\mathbf{H}\|b$	1.96 ± 0.15	160 ± 10
	$\mathbf{H}\perp(10\bar{2})$	2.36 ± 0.15	157 ± 10
	$\mathbf{H}\|[201]$	1.96 ± 0.15	159 ± 10
$T=4.2$ K	$\mathbf{H}\|b$	1.5 ± 0.1	154 ± 6
	$\mathbf{H}\perp(10\bar{2})$	1.6 ± 0.3	140 ± 20
	$\mathbf{H}\|[201]$	1.4 ± 0.1	148 ± 8

of the singlet-triplet transitions, taken at different orientations, should origin from one of these three values. At $g\mu_B H\gg D,E$ the asymptotic field dependence of the low-frequency singlet-triplet transition may be derived from Eq. (3):

$$\hbar\omega=\Delta-g_\alpha\mu_B H+\frac{D}{2}[(\mathbf{z}\cdot\mathbf{n})^2+1]+\frac{E}{2}[(\mathbf{x}\cdot\mathbf{n})^2-(\mathbf{y}\cdot\mathbf{n})^2]. \tag{11}$$

Thus, the measured values of $\tilde{\Delta}$ for different orientations should differ for about ±5 GHz. This shift is within the experimental resolution for the value of $\tilde{\Delta}$ obtained from the frequency of line "*d*."

From the frequency-field dependences for the singlet-triplet absorption we determine the critical field H_c as a field, at which the singlet-triplet transition frequency turns to zero. These values measured at $T=1.5$ K are: $H_c(\mathbf{H}\|b)=58.3\pm1.0$ kOe, $H_c[\mathbf{H}\perp(10\bar{2})]=47.5\pm1.5$ kOe, and $H_c(\mathbf{H}\|[201])=58\pm2$ kOe. These values are in agreement with magnetization and specific-heat data.[6,11]

The value of $\tilde{g}$ measured at $T=1.5$ K coincides well with the g-factor values determined from the ESR of the thermally activated triplets. However, at $T=4.2$ K the slope of $f(H)$ dependence becomes smaller for the factor of 0.75, while the value of $\tilde{\Delta}$ obtained from the extrapolation to zero field remains constant within the experimental error of 10%. Thus the increase of the critical-field value at the increase of temperature should be ascribed to a change of the field influence on the singlet-triplet gap and not to the change of the zero-field gap Δ. It is important to note here that the value of $\tilde{g}$ is temperature dependent, but the g factor describing the field dependence of the sublevels of the excited triplets does not depend on the temperature. The change of the effective g factor $\tilde{g}$ may be presumably attributed to the effect of the thermal renormalization of magnon frequency observed for the related compound $KCuCl_3$.[23]

C. Magnetic resonance in the field-induced magnetically ordered phase

The component "*e*" of the ESR line observed at $H>H_c$, shown in Fig. 3, demonstrates nonlinear and anisotropic spectrum presented on Figs. 8–10 and constitutes an antiferromagnetic resonance mode. The relative difference in resonance fields measured for different orientation of the

sample in this field range is much larger than the relative change in g factors in the paramagnetic phase. This essential anisotropy marks the spontaneous symmetry breaking due to the magnetic ordering above H_c.

No theory of the antiferromagnetic resonance in the field-induced antiferromagnetic phase is developed yet. The theory should consider the unsaturated order parameter which is induced by the magnetic field. Possible longitudinal oscillations of the order parameter should be taken into account.

We propose here a simplified treatment of the observed mode based on a molecular-field model, see, e.g., Ref. 24. This model appeared to be adequate for the description of spin-resonance modes in most conventional antiferromagnets, as well as in impurity-induced ordered phases of spin-gap magnets.[25,26] According to this model, antiferromagnetic resonance modes correspond to oscillations of the order parameter and magnetization, which are affected by the crystal-field anisotropy and external field. The antiferromagnetic resonance frequencies are determined by the exchange energy and by the anisotropy terms of the second order in the series expansion of the energy. For a monoclinic crystal the second-order terms have orthorhombic (two-axes) symmetry.[27] One of the symmetry axes of the second order anisotropy terms should be aligned along the twofold axis b. As at the above analysis of triplet ESR, we chose another axis along the easy-spin direction caused by the magnetic field in b direction—at an angle of 39° from a axis in the a-c plane.

Thus, for $\mathbf{H}\|b$ magnetic field lies along an anisotropy axis. For $\mathbf{H}\perp(10\bar{2})$ magnetic field is oriented at an angle of 77.6° with respect to the second anisotropy axis, and for $\mathbf{H}\|[201]$—at an angle of 12.4°. These angles are close to 90° and 0°, respectively, allowing an approximate description of the resonance spectra by the relations derived for exact orientations. There are two branches of the antiferromagnetic resonance absorption.[24] In the high-field range above the spin-flop transition, the first branch has the frequency, approaching to the paramagnetic resonance frequency, and the frequency of the second branch does not depend on the field (under the assumption of constant sublattice magnetization):

For **H** parallel to the hard axis of anisotropy,

$$f_1=\sqrt{(\gamma H)^2+C_2^2}, \tag{12}$$

$$f_2=C_1. \tag{13}$$

For **H** parallel to the second-easy axis of anisotropy,

$$f_1=\sqrt{(\gamma H)^2+C_1^2}, \tag{14}$$

$$f_2=C_2. \tag{15}$$

For **H** parallel to the easy axis and above the spin-flop field,

$$f_1=\sqrt{(\gamma H)^2-C_1^2}, \tag{16}$$

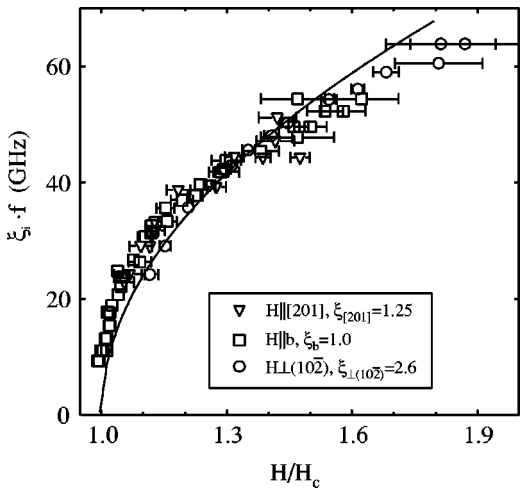

FIG. 14. Normalized frequency-field dependences of the antiferromagnetic resonance for three directions of the magnetic field. Solid curve is the fitting result (see text).

$$f_2=\sqrt{C_2^2-C_1^2}. \tag{17}$$

Here $C_2>C_1$, $C_i=\sqrt{2H_{Ai}H_E}/\gamma$, γ is magnetomechanical ratio, H_{Ai} and H_E are two effective anisotropy fields and exchange field, respectively. Each of the values H_{Ai} and H_E is proportional to sublattice magnetization, hence to the order parameter.

The branch f_1 has the frequency beyond our range 80 GHz in fields above 50 kOe. Thus we conclude that the resonance frequency in the high-field phase of $TlCuCl_3$ corresponds to the branch f_2 of a two-axes antiferromagnet. The observed field dependence of resonance frequencies should be ascribed to the specific nature of the field-induced ordering, when the order parameter is induced by the magnetic field and rises from zero at $H=H_c$. Hence we suppose the resonance frequency observed at $H>H_c$ is a measure of the field-induced order parameter.

This treatment suggests a universal dependence of normalized resonance frequency on the normalized field. The universality takes place indeed: as shown on the Fig. 14, three normalized frequency-field dependences taken for different field orientations coincide well. The normalization factors for resonance frequency are: 1.0 for $\mathbf{H}\|b$, 1.25 for the $\mathbf{H}\|[201]$, and 2.6 for the $\mathbf{H}\perp(10\bar{2})$. The normalized magnetic field was calculated using the values of H_c for different field orientations obtained from the analysis of the singlet-triplet transitions in the preceding section.

The measured antiferromagnetic resonance frequencies, and hence the order parameter m, follow a square-root dependence on the magnetic field (solid line on the Fig. 14):

$$f=C\sqrt{\frac{H}{H_c}-1} \tag{18}$$

The above consideration of the field-induced order parameter is consistent with the results of the neutron-scattering

experiments[8] performed for $\mathbf{H}\|b$, where the square root field dependence of the order parameter was also confirmed near H_c.

V. CONCLUSIONS

The detailed ESR study of the spin-gap compound $TlCuCl_3$ revealed three kinds of magnetic-resonance signals.

Different kind of magnetic excitations not reported before is the antiferromagnetic resonance mode in the field-induced ordered phase. This branch of spin excitations demonstrates nonlinear and strongly anisotropic spectrum. From the spectrum of this branch, in the molecular-field approximation, we deduce that the field-induced order parameter has a universal dependence for all directions of the magnetic field: $m \propto \sqrt{H-H_c}$. This spin-resonance mode indicates an important role of the crystal anisotropy in the formation of the order parameter in the high-field phase. The anisotropy fixes the direction of the transverse order parameter, breaking the rotational symmetry around the direction of the magnetic field. Hence, the BEC model, implying the rotational symmetry, has a limited applicability to $TlCuCl_3$, giving the description of the exchange effects, but neglecting the influence of the crystal field.

Second, we have observed direct ESR transitions between the singlet ground state and excited triplet states. The negative field-dependent contribution to the singlet-triplet transition frequency is temperature dependent. The nature of this temperature dependence is probably due to the thermal renormalization of the magnon frequencies. The quantitative theory of this renormalization is to be constructed.

Third, we found magnetic-resonance signals of thermally activated triplet excitations, and measured the crystal-field splitting of their spin sublevels. The effective energy of the interaction between the triplet excitations and the crystal field is obtained. The formation of the exchange narrowed collective resonance mode of the interacting triplet excitations was observed.

ACKNOWLEDGMENTS

Authors acknowledge to A. N. Vasil'ev, A. K. Kolezhuk, M. E. Zhitomirsky, V. I. Marchenko, S. S. Sosin for discussions. The work was supported by the Russian Foundation for Basic Research Grant No. 03-02-16579.

*Electronic address: glazkov@kapitza.ras.ru

[1] M. Hase, I. Terasaki, and K. Uchinokura, Phys. Rev. Lett. **70**, 3651 (1993).
[2] L.P. Regnault, I. Zaliznyak, J.P. Renard, and C. Vettier, Phys. Rev. B **50**, 9174 (1994).
[3] E. Dagotto and T.M. Rice, Science **271**, 618 (1996).
[4] H. Kageyama, K. Yoshimura, R. Stern, N.V. Mushnikov, K. Onizuka, M. Kato, K. Kosuge, C.P. Slichter, T. Goto, and Y. Ueda, Phys. Rev. Lett. **82**, 3168 (1999).
[5] L.P. Regnault, J.P. Renard, G. Dhalenne, and A. Revcolevschi, Europhys. Lett. **32**, 579 (1995).
[6] A. Oosawa, M. Ishi, and H. Tanaka, J. Phys.: Condens. Matter **11**, 265 (1999).
[7] A. Oosawa, T. Ono, and H. Tanaka, Phys. Rev. B **66**, 020405(R) (2002).
[8] H. Tanaka, A. Oosawa, T. Kato, H. Uekusa, Y. Ohashi, K. Kakurai, and A. Hoser, J. Phys. Soc. Jpn. **70**, 939 (2001).
[9] N. Cavadini, G. Heigold, W. Henggeler, A. Furrer, H.-U. Güdel, K. Krämer, and H. Mutka, Phys. Rev. B **63**, 172414 (2001).
[10] A. Oosawa, T. Kato, H. Tanaka, K. Kakurai, M. Müller, and H.-J. Mikeska, Phys. Rev. B **65**, 094426 (2002).
[11] A. Oosawa, H. Aruga Katori, and H. Tanaka, Phys. Rev. B **63**, 134416 (2001).
[12] T. Nikuni, M. Oshikawa, A. Oosawa, and H. Tanaka, Phys. Rev. Lett. **84**, 5868 (2000).
[13] H. Tanaka, T. Takatsu, W. Shiramura, T. Kambe, H. Nojiri, T. Yamada, S. Okubo, H. Ohta, and M. Motokawa, Physica B **246-247**, 545 (1998).
[14] K. Takatsu, W. Shiramura, H. Tanaka, T. Kambe, H. Nojiri, and M. Motokawa, J. Magn. Magn. Mater. **177-181**, 697 (1998).
[15] Ch. Rüegg, N. Cavadini, A. Furrer, H.-U. Güdel, K. Krämer, H. Mutka, A. Wildes, K. Habicht, and P. Vorderwisch, Nature (London) **423**, 62 (2003).
[16] A. Abragam and B. Bleaney, *Electron Paramagnetic Resonance of Transition Ions* (Clarendon, Oxford, 1970).
[17] P.W. Anderson, J. Photogr. Sci. **9**, 316 (1954).
[18] D.B. Chestnut and W.D. Phillips, J. Chem. Phys. **35**, 1002 (1961).
[19] V.N. Glazkov, R.M. Eremina, A.I. Smirnov, G. Dhalenne, and A. Revcolevschi, Zh. Éksp. Teor. Fiz **120**, 164 (2001) [JETP **93**, 143 (2001)].
[20] A.I. Smirnov, V.N. Glazkov, and S.S. Sosin, Pis'ma Zh. Eksp. Teor. Fiz. **77**, 517 (2003) [JETP Lett. **77**, 442 (2003)].
[21] M. Date and K. Kindo, Phys. Rev. Lett. **65**, 1659 (1990).
[22] L-P. Regnault, I.A. Zaliznyak, and S.V. Meshkov, J. Phys.: Condens. Matter **5**, L677-L684 (1993).
[23] N. Cavadini, Ch. Rüegg, W. Henggeler, A. Furrer, H.-U. Güdel, K. Krämer, and H. Mutka, Eur. Phys. J. B **18**, 565 (2000).
[24] T. Nagamiya, K. Yosida, and R. Kubo, Adv. Phys. **4**, 1 (1955).
[25] V.N. Glazkov, A.I. Smirnov, K. Uchinokura, and T. Masuda, Phys. Rev. B **65**, 144427 (2002).
[26] A.I. Smirnov, V.N. Glazkov, H.-A. Krug von Nidda, A. Loidl, L.N. Demianets, and A.Ya. Shapiro, Phys. Rev. B **65**, 174422 (2002).
[27] A.N. Vasil'ev, V.I. Marchenko, A.I. Smirnov, S.S. Sosin, H. Yamada, and Y. Ueda, Phys. Rev. B **64**, 174403 (2001).